Hindawi
Shock and Vibration
Volume 2018, Article ID 4932870, 12 pages
https://doi.org/10.1155/2018/4932870

Research Article

Particle Swarm Optimization for Active Structural Control of Highway Bridges Subjected to Impact Loading

Jake Edmond Hughes,[1] Yeesock Kim,[2] Jo Woon Chong,[3] and Changwon Kim[4]

[1]*Department of Civil and Environmental Engineering, Worcester Polytechnic Institute (WPI), Worcester, MA 01609, USA*
[2]*Department of Civil Engineering and Construction Management, California Baptist University (CBU), Riverside, CA 92504, USA*
[3]*Department of Electrical and Computer Engineering, Texas Tech University, Lubbock, TX, USA*
[4]*Daegu Research Center for Medical Devices and Rehabilitation Engineering, Korea Institute of Machinery and Materials, Daegu 42994, Republic of Korea*

Correspondence should be addressed to Yeesock Kim; yekim@calbaptist.edu

Received 28 February 2018; Revised 23 May 2018; Accepted 27 June 2018; Published 14 August 2018

Academic Editor: Adam Glowacz

The application of active structural control technology to highway bridge structures subjected to high-impact loadings is investigated. The effects of high-impact loads on infrastructure, like heavy vehicle collisions with bridge piers, have not been studied as much as seismic load effects on structures. Due to this lack of research regarding impact loads and structural control, a focused study on the application of active control devices to infrastructure after impact events can provide valuable results and conclusions. This research applies active structural control to an idealized two-span, continuous girder, concrete highway bridge structure. The idealization of a highway bridge structure as a two degree-of-freedom structural system is used to investigate the effectiveness of control devices installed between the bridge pier and deck, the two degrees of freedom. The control devices are fixed to bracing between the bridge pier and girders and controlled by the proportional-integral-derivative (PID) control. The PID control gains are optimized by both the Ziegler–Nichols ultimate sensitivity method (USM) and a new method for this impact load application called particle swarm optimization (PSO). The controlled time-domain responses are compared to the uncontrolled responses, and the effectiveness of PID control, USM optimization, and PSO is compared for this control device configuration. The results of this investigation show PID control to be effective for minimizing both superstructure and substructure responses of highway bridges after high-impact loads. Deck response reductions of greater than 19% and 37% were seen for displacement and acceleration responses, respectively, regardless of the performance index used to analyze them. PSO was much more effective than USM optimization for tuning PID control gains.

1. Introduction

1.1. Control Technology for Structural Impact Mitigation. Recently, control technology has been proposed and applied to large civil structures in order to deal with the effects of seismic and wind loadings [1–3]. The mitigation of excessive structural vibration, displacement and/or accelerations, and therefore, damage is the purpose of control technology for civil infrastructure [4]. In order to effectively utilize control devices in civil infrastructure, system dynamics models need to be developed that include the control system dynamics and the interaction between the control device and the structure [5–15]. Much progress has been made in proposing active control algorithms for seismic applications [6, 8–10, 16–18].

One area of control technology research in civil structures that has received less attention than seismic research is the problem of high-impact loading [13–15]. High-impact loads can be caused by aircraft, marine vessels, or large vehicle collisions with civil infrastructure, most commonly bridges and buildings. Structures excited by impact loads often exhibit nonlinear material behavior, large deformation responses, and instability. These complex behaviors can lead to insufficient life safety and even structural collapse [16].

Ongoing impact load research in the civil engineering domain focuses in part on finite element analysis of vessel crushing behavior, its effects on bridge structures, and how those effects are accounted for in the AASHTO design code [17]. It is the purpose of this research to demonstrate effective structural control of a highway bridge structure after an impact load and also optimize the proportional-integral-derivative (PID) control of this structure. The time-history response of the structure after the applied impact load will provide valuable information about the effectiveness of active structural control in this application and guide future research in the area.

1.2. Relevant Background. Recently, the structural engineering field has seen a great increase in research focused on active and semi-active structural control. Unlike passive structural control through tuned mass dampers, tuned liquid dampers, and similar devices, active structural control involves the sensing of structural response and the use of that information in real time to put control forces into the structure through actuators. Active structural control can be more effective than passive structural control because of its ability to rapidly and continuously adjust control forces imparted on the structure using a computer [5, 8].

In order to effectively use control devices in civil engineering structures like bridges, the control system design must be optimized. This involves the choice and optimization of controllers like the PID, LQG, LQR, and fuzzy controllers. The use of these specific controllers and optimization of their parameters for structures under seismic loads have been widely studied [16, 18–23]. The use of these controllers, and comparison of performance, has not yet been widely applied to the high-impact load problem. This research paper describes the complete control system design and tuning for a highway bridge structure employing control devices subjected to a high-impact load on one of its piers. The uncontrolled and PID-controlled responses of the bridge structure are compared in order to investigate the effectiveness of active structural control after high-impact loads. The bridge design and controller use for the proposed research will be based on similar research papers dealing with seismic excitation forces.

In order to develop a structural formulation and design for this research, the 2002 paper "Investigation of semi-active control for seismic protection of elevated highway bridges" [24] was studied. In this research, active, passive, and semi-active control system performance is compared for elevated highway bridges subjected to seismic loading. The elevated highway bridges had piers of identical properties supporting a bridge deck on rubber bearings. The control devices were attached to the top of the piers and bottom of the bridge deck. This created a two degree-of-freedom model of the structure. The system was represented in state-space form, and the LQR control strategy was used for active and semi-active control of the structure for the El-Centro, Kobe, and Northridge earthquakes. Displacement time-history responses were compared to come up with results and conclusions. This research showed that increasing damping for the passive control case decreased structural response for both the pier and deck only until a certain damping level. The active control case was effective when designed for either the deck or pier response minimization but did not achieve results better than the passive case when designed for both DOF minimization.

Similar research was carried out by Yan and Zhang in their paper "Smart vibration control analysis of seismic response using MR dampers in the elevated highway bridge structures." [23] In this research, a similar problem formulation was used, but the study focused on evaluating the effectiveness of the rubber bearing plate-MR damper combination in the bridge structure. In one system, the MR dampers connected the piers to the girders of the bridge, and in the other proposed system, the MR dampers were placed between the bridge girders. The state-space formulation and LQR controller were used for analysis, and the results were given in terms of acceleration and displacement reduction.

Impact load studies with active/semi-active control devices are still not as prevalent as seismic load research [14, 15, 25, 26]. Li and Wang [25] experimentally investigated the effectiveness of PID control of a large MR shock absorber subjected to high-impact loading. Although the proposed research will focus on simulations and active control, it is still valuable to see similar experimental applications, especially because this specific application deals with impact loading. This paper used a P, PI, and PID controller to mitigate the peak response of the MR shock absorber with an applied impact load. The comparative time-history responses showed that P control was the most effective control case for minimizing peak impact response. The optimization of PID control gains was not a part of this research paper. Arsava and Kim [26] applied the semi-active fuzzy logic-based controller to reinforced concrete structures equipped with MR dampers in order to mitigate structural impact responses.

The previous research related to this topic described above provides the theoretical framework and rationale for the investigation of optimal PID controller selection for highway bridge structure damage mitigation due to high-impact loads. The modelling of the bridge structures as two degree-of-freedom mass-spring models and the use of the state-space formulation for simulation are what the proposed research will entail [27]. Instead of seismic loading, a finite element-produced impact load will be used for simulation input.

The remaining sections of this paper include a description of the physical system and approach in Section 2, the simulation results and analysis in Section 3, and the summary of results and conclusions in Section 4.

2. Proposed System and Approach

2.1. State Space Model. In order to effectively investigate the effects of high-impact loads on highway bridge structures, a physical system was defined. Typical highway bridge structures usually consist of piers, bearings, and a superstructure that includes the girders and bridge deck. For multispan highway bridge structures, it is often the case

that each pier has similar dimensions and characteristics to the other piers. In this case, the system can be easily defined as a single degree-of-freedom system with the lumped mass bridge piers and superstructure located at the top of the piers. This simplified model has been shown to provide useful information for dynamic analysis because it is reasonable to model the bridge deck superstructure as a rigid body. A slightly more complicated, but still simple, highway bridge structure model involves two degrees of freedom, the bridge pier and the deck. In this model, the top of the bridge pier and bridge deck represent two degrees of freedom that communicate through the bearing plates between them [24]. In this model, passive control by either friction of the bearing material or installed passive control devices can be studied simply using an associated stiffness and damping of the bearing plate. Active and semiactive control can also be studied using this two degree-of-freedom model by installing the control devices between the top of bridge piers and the bottom of the deck. The idealized two degree-of-freedom structural model chosen for this research is shown in Figure 1. The impact load F_I is applied to the bridge pier, and control devices with the corresponding control force F_C act between the sub- and superstructure. Although the model is simple, it has the ability to provide useful and important information about the response of highway bridge structures to impact loads. The interaction between the bridge deck and pier through the control device is the most important benefit of the two degree-of-freedom system over its single degree-of-freedom counterpart.

The model parameters are summarized in Table 1. A 150 ft long two-span concrete structure was chosen as the typical small highway bridge structure for investigation. The natural period of the structure was assumed to be 0.5 seconds, and the damping ratio of the pier was set to 0.05, both typical values for highway bridge structures [24]. The masses of the deck and pier were set based on the volume of normal weight concrete. In order to generate reasonable results, the bearing plate parameters were set to feature very low damping and moderate stiffness.

In addition to the definition of the above parameters, an impact load was determined and applied to the model at the first, bridge pier, degree of freedom. This impact load was defined as a 66 kN Ford delivery truck impacting the bridge pier at approximately 90 kph. This vehicle was used because of its size, prevalence on both highways and smaller volume roadways, and its use in previous finite element model research. El-Tawil et al. [28] built a finite element model of this vehicle and subjected it to bridge pier impact under the aforementioned conditions. The impact load curve generated by their simulations was used in this research to apply to the bridge pier. The peak force from the impact load curve was approximately 3000 kN, and the start-to-end load duration was approximately 0.25 seconds. This impact load was chosen to be used over laboratory drop tower impact load tests because it accounted for the nonlinear crushing behavior of the vehicle and therefore was a more accurate representation of the load that the pier would face. This model assumes that the impact force does not cause a critical instability in the bridge pier and that the pier remains relatively undamaged throughout the response. These assumptions are acceptable for the purposes of examining the effectiveness of PID-controlled devices on minimizing structural response and comparing the effectiveness of the USM and PSO tuning techniques.

The state-space formulation was used to define the structural system, and PID control was implemented using MATLAB/Simulink. The system represented in state-space form is as follows:

$$\begin{aligned} \dot{\mathbf{X}} &= \mathbf{AX} + \mathbf{Bu}, \\ \mathbf{y} &= \mathbf{CX} + \mathbf{Du}, \end{aligned} \tag{1}$$

where $\mathbf{X}$ is the state vector, $\mathbf{u}$ is the input vector, $\mathbf{A}$ is the system matrix, and $\mathbf{B}$ is the input matrix. The output of the state-space form is $\mathbf{y}$, the output matrix is $\mathbf{C}$, and the $\mathbf{D}$ matrix was assumed null.

2.2. PID Controller. Dynamic response improvement can be achieved using a PID controller. PID control has been used in approximately 90% of industrial processes across the world [29] and has also been shown to be effective for structural control purposes [30]. In this controller, the sensed error from a set reference point is operated on by proportional, integral, and derivative terms in order to generate control signals that animate devices in the structure to minimize its response. The proportional term counters large errors with large output, the integral term eliminates steady-state errors, and the derivative term smoothes quickly changing error. In general, for processes that respond quickly to a controller, the integral term will be smaller and the derivative term larger since errors changes sign rapidly. A simple PID controller is described as follows in (2):

$$v(t) = K_P y(t) + K_I \int_0^t y(t)dt + K_D \frac{dy(t)}{dt}, \tag{2}$$

where $v(t)$ is the time-dependent control signal; $y(t)$ is the structural responses; and K_P, K_I, and K_D are the proportional, integral, and derivative control gains, respectively.

2.3. Ultimate Sensitivity Method. The initial optimization of PID control gains, for bridge deck displacement and acceleration minimization, was completed using the ultimate sensitivity method (USM) based on the Ziegler–Nichols tuning rules for automatic controllers [31]. This method is widely used and can be described as a bridge between strict trial and error type approaches and analytical approaches to optimizing PID control gains. The method was designed to achieve acceptable responses after disturbances to the system [32]. The USM involves finding the lowest proportional control gain such that the system just oscillates (K_m), determining its accompanying natural frequency (ω_n), and then using (3)–(5) below to define the three tuned PID control gains. While this method was not developed for impact loading of civil infrastructure and is often used to "get close" the optimum control solutions, it will be used as

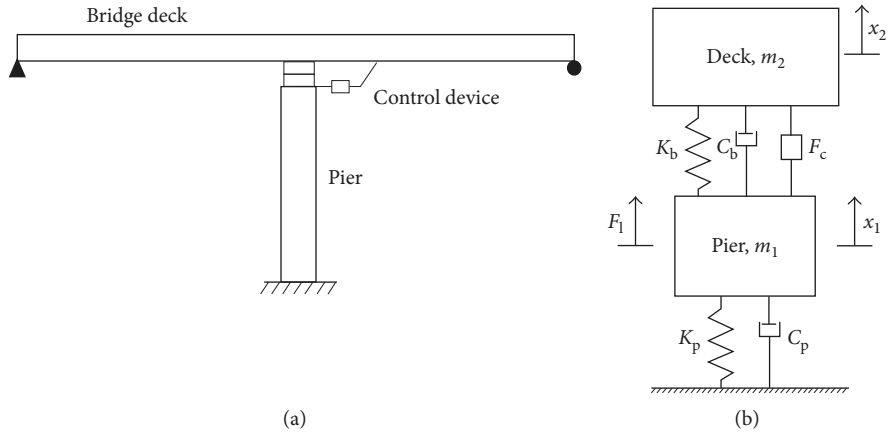

Figure 1: (a) Idealized two-span highway bridge structure and (b) idealized two degree-of-freedom model for impact loading.

Table 1: Model physical parameters.

Parameter	Value
Deck mass, m_2	1.53×10^6 kg
Pier mass, m_1	3.1×10^5 kg
Deck damping ratio, C_b	0.01
Pier damping ratio, C_p	0.05
Pier natural period, ω_p	0.5 sec
Stiffness ratio (pier/deck), K_p/K_b	2

a baseline comparison for optimal PID control for this research.

$$K_P = 0.6K_m, \tag{3}$$

$$K_I = \frac{K_P \omega_n}{\pi}, \tag{4}$$

$$K_D = \frac{\pi K_P}{4\omega_n}. \tag{5}$$

With the above equations as reference points, a more rigorous optimization approach was used to calculate the optimized proportional, integral, and derivative control gains. This approach was particle swarm optimization (PSO).

2.4. Particle Swarm Optimization

2.4.1. Introduction. Particle swarm optimization, an effort to produce computational intelligence by using social interaction referents, was introduced in 1995 [33]. Since being introduced, many papers have been published examining the PSO algorithm itself, the effects of modifying different tuning parameters, enhancing the algorithm, and the use of PSO for various types of optimization problems [34–36]. The PSO algorithm features very stable convergence and has been shown to achieve excellent results with shorter calculation times compared with other stochastic algorithms [34, 37].

2.4.2. Concept and Use. The particle swarm methodology, based on social and psychological principles, was developed for the optimization of nonlinear functions [38]. The use of the term "swarm" by Kennedy and Eberhart is based on swarm intelligence and an outline of its five basic principles [39]. These principles include proximity, quality, diverse response, stability, and adaptability. Bird flocking and fish schooling are common behaviors cited to explain particle swarm methodology [33]. The PSO algorithm is related to genetic algorithms and evolutionary computing, but it is based on the assumption that an advantage is gained with the social sharing of information among members of the swarm. Unlike genetic algorithms that mimic natural selection, PSO algorithms utilize swarm memory and group interactions to improve the proposed solution over time. This means that PSO can be used to solve similar problems to genetic algorithms, but it has some clear advantages. All population members typically survive in the entire iterative process in PSO, unlike in genetic algorithms based on natural selection; this maintains previous problem knowledge throughout the entire simulation [38]. Also, since group interaction occurs in the swarm, the system memory is retained by all particles in the group, thus leading to less loss of information and lowered likelihoods of missed optima.

The PSO algorithm has been implemented for many different applications including logic circuit design, control design, power systems design, structural shape optimization, and topology optimization, among others [40]. Figure 2 shows photographs representing specific examples of the use of the PSO algorithm that ranges from the detection and classification of human wrist tremors to the multiobjective design of aircraft wings [41, 42]. PSO techniques have also been used for PID control gain tuning [43], but not for impact loading applications in civil engineering.

The PSO algorithm is strong in dealing with high dimensionality, nonlinear problems, nondifferentiability, and problems with several optima [43]. It is easy to implement and has good computational efficiency [35]. Other evolution-based computational methods use operators to manipulate individual particles. PSO, on the other hand, adjusts an individual particle's velocity based on its self-experience and the experiences of its nearest neighbors. The individual particles that make up the swarm fly around the n-dimensional search space looking for optimum solutions. Coordinates are tracked and velocities are adjusted based on

Figure 2: Photographs of specific examples of the use of PSO techniques (published and labelled for reuse by wikipedia.org and pixabay.com).

the best solutions found in each generation, or time step, of the algorithm. Particle velocities are changed to pull the particles toward local optimum solutions ($\mathbf{p}_i$) and a global optimum solution ($\mathbf{p}_g$). Once a sufficient number of generations have passed, the swarm will have converged on optimum coordinates, and the overall best result will be reported.

2.4.3. Basic PSO Algorithm. In the PSO algorithm, the location vector of the ith particle in n-dimensional space at time t is represented as $\mathbf{x}_i^t = (x_{i,1}^t, x_{i,2}^t, \ldots, x_{i,n}^t)$. The best previous location of that particle is $\mathbf{p}_i = (p_{i,1}, p_{i,2}, \ldots, p_{i,n})$, and the best previous particle location among all particles in the swarm, or group, is given by $\mathbf{p}_g = (p_{g,1}, p_{g,2}, \ldots, p_{g,n})$. The adjusted velocity and location of each particle are based on the previous velocity of the particle and its distance from the individual and group best locations as follows:

$$\mathbf{v}_i^{(t+1)} = w\mathbf{v}_i^{(t)} + a_1 r_1 \frac{\left(\mathbf{p}_i - \mathbf{x}_i^{(t)}\right)}{\Delta t} + a_2 r_2 \frac{\left(\mathbf{p}_g - \mathbf{x}_i^{(t)}\right)}{\Delta t}, \quad (6)$$

$$\mathbf{x}_i^{(t+1)} = \mathbf{x}_i^{(t)} + \mathbf{v}_i^{(t+1)} \Delta t, \quad i = 1, 2, \ldots, k, \quad (7)$$

where k is the number of particles in the swarm, t is the generation, w is an inertial weighting factor, a_1 and a_2 are acceleration constants, $\mathbf{v}_i^{(t)}$ is the velocity of particle i at generation t, $\mathbf{x}_i^{(t)}$ is the current position of the particle i at generation t, and r_1 and r_2 are random numbers between 0 and 1. The progression of a single particle from generation t to generation $t + 1$ is shown graphically using vectors and nodes in Figure 3. Figure 3(a) is annotated with detailed descriptions, while Figure 3(b) is annotated using expressions from (6) and (7).

In the PSO algorithm, maximum and minimum values for particle velocity are set to ensure that particles do not fly over good solutions or not sufficiently explore the entire workspace for better solutions. Random starting locations are often used and the acceleration weighting constants control the abruptness of movement toward target regions. These constants represent the "confidence" or trust that an individual particle has with its own previous best experience compared with that of the swarm overall. The inertial weighting criteria balance the global and local exploration characteristics of each particle in the swarm by acting on the initial velocity. The basic PSO model works in the followings steps:

Step 1: An array of particles is created with random positions and velocities in n-dimensions

Step 2: The objective function is identified and evaluated in the n-dimensions for each particle

Step 3: Each evaluation is compared to the previous best value for the individual particles separately; if the current evaluation is better than the previous best, it takes the place of the previous best value in individual particle memory

Step 4: Each evaluation is compared to the previous best value for the swarm; if the current evaluation is better than the previous best, it takes the place of the previous best value in the overall swarm memory

Step 5: Individual particle velocity is changed by (6)

Step 6: Individual particle location is changed by (7), reset the current generation, loop to the second half of step 2 (evaluation of objective function), and repeat until a convergence criterion is met

2.4.4. Further Details and Enhancements to the PSO Algorithm. In addition to the basic PSO algorithm, various enhancements and changes have been proposed and made by researchers over time. The population topology or control of proposed solutions throughout the problem has been adjusted in various ways. The original is the *gbest* topology in which all particles are connected to all other particles, and the population is fully connected. An *lbest* topology was proposed as a modification in order to achieve better results in the case of sparse topology with various local optima. This topology has each particle only connected to its nearest neighbors in a ring lattice-type structure. It was shown to converge more slowly, but also more accurately in regions with various local optima [38].

In addition to the gbest and lbest topologies, inertial weight updates over generations in the algorithm have been proposed to improve global to local search behavior. Both a linear decrease of w with each algorithm iteration [44] and a decrease of w based on a fractional multiplier [45] have been proposed to search globally at the start of the algorithm and focus locally after many iterations.

After the combination of (6) and (7), the rearranging of certain terms, and putting them into matrix form, the following convergence and stability conditions are achieved [40]. The condition for convergence is that which describes an equilibrium point, $\mathbf{v}_i^t = 0$, $\mathbf{x}_i^t$, and $\mathbf{p}_i$ coincide with $\mathbf{p}_g$.

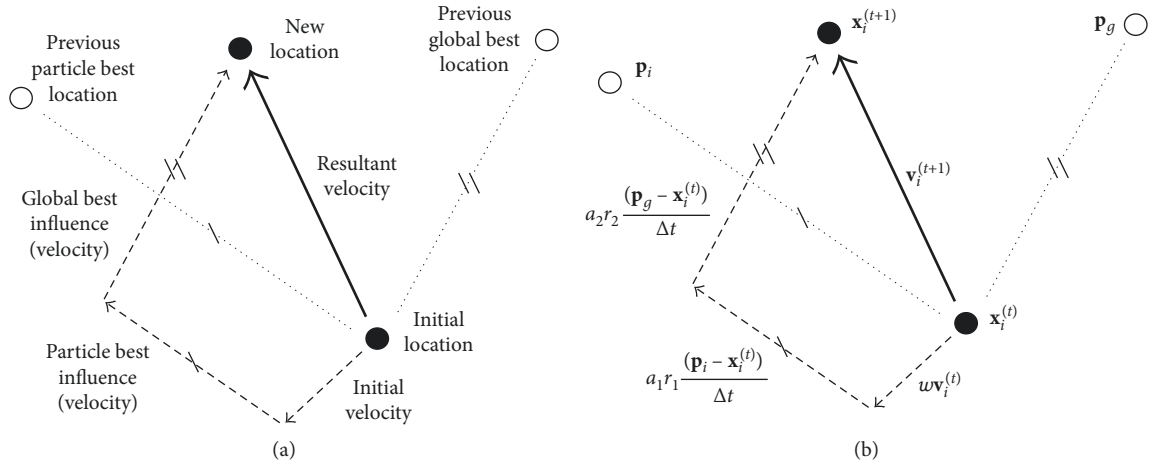

Figure 3: (a) Particle progression description. (b) Equations (6) and (7) expression format.

If better positions are found, this equilibrium configuration is disturbed. Practically, it is often the case that a maximum change in the objective function is monitored for each design iteration. If this change falls below a certain user-set tolerance, convergence is deemed to have occurred and the algorithm stopped [35]. The stability conditions, or eigenvalues, derived from the matrix form equation are as follows:

$$a_1r_1 + a_2r_2 > 0,$$
$$\frac{a_1r_1 + a_2r_2}{2} - w < 1, \tag{8}$$
$$w < 1.$$

With some rearranging of terms and constraints on the random numbers, the following equations can be derived for parameter selection for PSO stability. As long as the following equations are satisfied, convergence to an equilibrium point is guaranteed [40].

$$0 < a_1 + a_2 < 4,$$
$$\frac{a_1 + a_2}{2} - 1 < w < 1. \tag{9}$$

Although the PSO algorithm is defined for unconstrained problems, it is often the case that engineering applications require or favor the use of constraints. An adaptive penalty scheme has been proposed such that nonviable solutions are adjusted by a penalty parameter [40]. The scheme is meant to decrease the favorability of nonviable solutions compared with the viable solutions. In addition to the penalty scheme for nonviable solutions, the redirection of particle velocities away from nonviable design spaces was introduced [35]. This redirection is achieved by modifying the updated velocity equation (6) to the form of (10). This equation has the initial velocity and inertial weight term removed.

$$\mathbf{v}_i^{(t+1)} = a_1r_1\frac{\left(\mathbf{p}_i - \mathbf{x}_i^{(t)}\right)}{\Delta t} + a_2r_2\frac{\left(\mathbf{p}_g - \mathbf{x}_i^{(t)}\right)}{\Delta t}. \tag{10}$$

This equation shows that the new velocity of the particle is no longer influenced by its inertia, and it is only influenced by the $\mathbf{p}_i$ and $\mathbf{p}_g$ locations. This modification has been shown to move the nonviable particle back toward the viable region of the design space. In cases where the particle remains nonviable after one iteration with the modified velocity algorithm, it is at least closer to the boundary in subsequent iterations [35]. The modified velocity algorithm and redirection enhancement are shown in Figure 4.

2.4.5. Proposed PSO Controller for Tuning PID Control Gains. The proposed PSO controller for PID tuning parameters was used according to the following basic outline:

Step 1. The upper and lower bounds of the three PID control gains were set, thus establishing the limits/constraints of the search space. A swarm size, maximum number of generations, and convergence tolerance were chosen for the optimization procedure.

Step 2. Particles are distributed randomly throughout the search space.

Step 3. The objective function in the algorithm was set as sum of the squared structural response over a specified time interval.

Step 4. Algorithm featuring (6) and (7) is run until the preset number of generations is reached, and then optimum K_P, K_I, and K_D values are reported.

The proposed analysis, outlined above, is shown in the block diagram in Figure 5.

2.5. Evaluation of Structural Response. In order to evaluate the performance of the PID controller for structural response minimization, two performance indices were used. The first was a comparison of the peak responses and the second an energy comparison method. The use of both of the following performance indices will provide a way to reason about the overall effectiveness of PID control, and the effectiveness of the USM and PSO tuning of control gains for bridge structures subjected to high-impact loads.

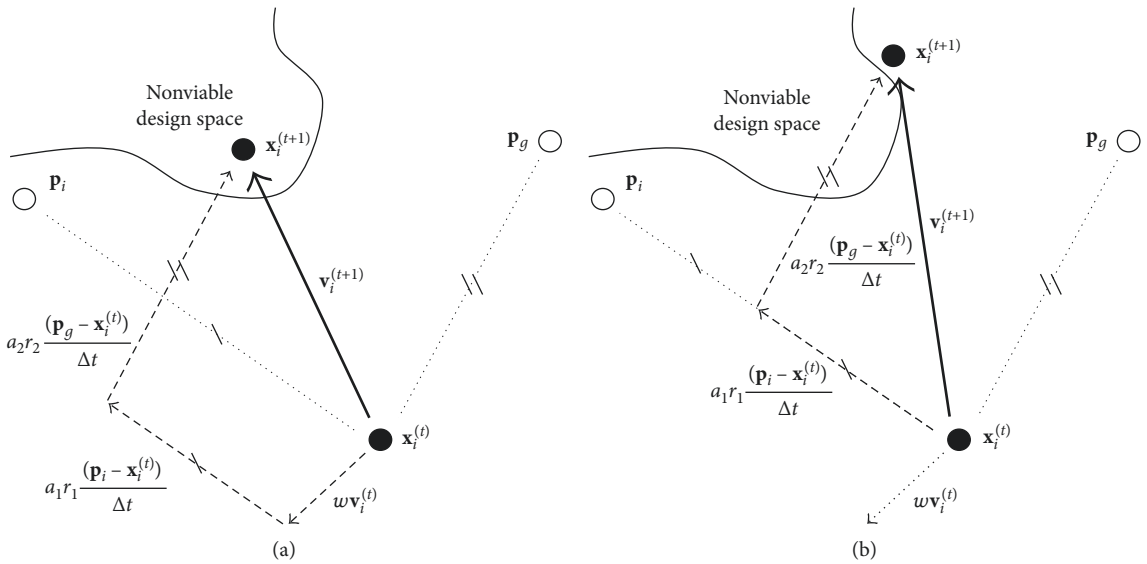

Figure 4: (a) Nonviable design space recognition and (b) correction to (6) and (7).

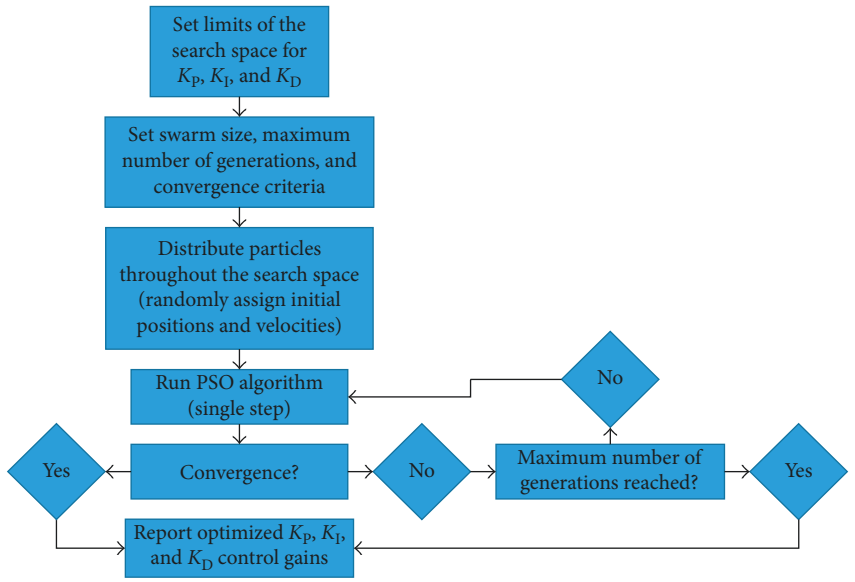

Figure 5: Proposed analysis block diagram.

Performance Index 1:

$$C_1 = \frac{\max(y_C)}{\max(y_{UC})}. \tag{11}$$

Performance Index 2:

$$C_2 = \sum \frac{|y_C|}{|y_{UC}|}, \tag{12}$$

where y_C is the controlled response of the structure and y_{UC} is the uncontrolled response of the structure. Both the displacement and acceleration responses for each degree of freedom were optimized and evaluated using these performance indices.

3. Simulation and Results Analysis

3.1. PID Control Gain Optimization by Ultimate Sensitivity. The optimization of PID control gains was completed by first using the ultimate sensitivity method, and then the PSO approach was used to investigate whether or not further refinements needed to be made to the control gains. After increasing the P control gain until the limit of stability for both the deck displacement and acceleration cases, the maximum P control gains were as shown in Table 2. Using the Ziegler–Nichols equations for PID control, the rest of Table 2 was filled out. This led to the setting of control gains shown in the bottom three rows of Table 2.

Table 2: Ultimate sensitivity method results.

Optimization case	Deck displacement	Deck acceleration	Pier displacement	Pier acceleration
Maximum control gain, K_M	10,000,000	500,000	1,000,000	50,000
Response period, T_n (sec)	1.65	1.8	2	2
Natural frequency, w_n (rad/s)	3.8	3.5	3.1	3.1
Proportional gain, K_P equation (3)	6,000,000	300,000	600,000	30,000
Integral gain, K_I equation (4)	7,272,800	333,270	600,000	30,000
Derivative gain, K_D equation (5)	1,237,500	67,510	150,000	7,500

3.2. PID Control Gain Optimization by Particle Swarm Optimization. The optimization of PID control gains was then completed using PSO. The swarm size, number of generations, and allowed bounds for the three objective control gains were preset and the simulations run. Using PSO for PID control gain optimization, Table 3 shows the results.

3.3. Impact Load Simulation Results. As described in Section 2.1, the impact force used in simulation had a peak of 3000 kN and a duration of 0.25 seconds. This impact load curve was generated by [28] using a finite element model of a 66 kN Ford delivery truck impacting a bridge pier at approximately 90 kph.

With the PID control gains specified by the ultimate sensitivity method and particle swarm optimization, the 15-second deck displacement and deck acceleration responses were compared to the uncontrolled structural responses visually. Based on these results, it was clear that the first 5 seconds of the simulated impact event was critical, so the 5-second impact responses were evaluated and compared quantitatively. The following results show significant response reduction for USM-PID-controlled bridge deck response as well as PSO-PID-controlled bridge deck response. Figures 6 and 7 show the optimized deck displacement and deck acceleration cases, respectively.

Figure 8 shows the deck moving over a peak-to-peak range of approximately 0.16 m for the uncontrolled case, 0.14 m for the USM-controlled case, and 0.11 m for the PSO-controlled case. It also shows significant response reduction after the initial peaks for both the USM- and PSO-controlled cases, with the PSO-controlled case reaching negligible structural motion around 5 seconds after impact. Figure 6 shows that PSO-PID control was as effective as the USM-PID control initially (0–0.5 s after impact), but that it performed much better than USM-PID control in the 0.5–5 s after the impact time period.

Figure 8 shows a typical required control force plot for each control method. As this plot is for the deck acceleration optimization case, it is not surprising that the PSO-PID required control force is slightly higher than the USM-PID-controlled case.

Figures 9 and 10 show the resulting responses of the bridge pier degree of freedom when optimizing for the deck responses in Figures 6 and 7, respectively.

Figure 9 shows that even when optimizing for deck displacement, the control devices cause minimization of motion for pier displacement as well. The exception to this rule in Figure 10 is that the initial peak for both USM- and PSO-controlled pier displacement cases is very similar, but slightly larger than the uncontrolled response. Like Figure 9, Figure 10 shows that even when optimizing for deck acceleration, the control devices cause the pier acceleration response to be lessened. In order to complete a thorough investigation of the effectiveness of the MR damper and USM and PSO techniques, pier displacement and pier acceleration optimization were also investigated. These results were analyzed in the same fashion as the results shown in Figures 6–10, and the results of all four completed optimization cases were quantified and are displayed in Table 4. Values showing no change or a reduction in response from the uncontrolled case are highlighted in green in these tables, while values that indicate response increases caused by the control devices are highlighted in orange. The first 5 seconds of displacement and acceleration response were used for these numerical results. The performance indices C_1 and C_2 are loosely referred to as response reduction ratios.

The top two rows of results in Table 4 compare the response reduction ratios for the USM and PSO technique based on the uncontrolled structural response. These rows show the response of both the deck and pier degrees of freedom through the use of performance indices C_1 and C_2 for the deck displacement optimization case. The "Deck C_1" column shows that the deck displacement response, measured by the peak value index C_1, was reduced to 87% of the uncontrolled response when the USM was used for the optimal PID control gains. It also shows that the deck displacement response, measured by C_1, was reduced to 81% of the uncontrolled response when PSO was used for the optimal control gains. This demonstrates that both control methods were effective at response minimization, but that PSO was significantly more effective at finding the optimal PID control gains. The second column "Deck C_2" shows similar results, but using the energy performance index C_2. The third and fourth columns show the resulting pier responses when optimizing PID control parameters for deck displacement. Interestingly, column three indicates that there is a tradeoff between minimizing deck displacement response and keeping the peak pier displacement low. This column indicates that in order to achieve the significant reductions in deck displacement shown in the first two columns, a small 1-2% increase in pier peak displacement must be allowed. This phenomenon was already mentioned and is shown in Figure 10, at the first downward peak location. Column four, unsurprisingly, shows that the pier displacement response, as measured by the energy index C_2, is still significantly reduced, even when optimizing for deck displacement.

The bottom four rows in Table 4 indicate that attempting to minimize pier response with the proposed damper

Table 3: Particle swarm optimization results.

Optimization case	Deck displacement	Deck acceleration	Pier displacement	Pier acceleration
Proportional gain, K_P	8,882,400	−901,650	3,940,900	98,850
Integral gain, K_I	−877,370	54,680	278,340	16,680
Derivative gain, K_D	2,157,700	161,620	194,430	22,020

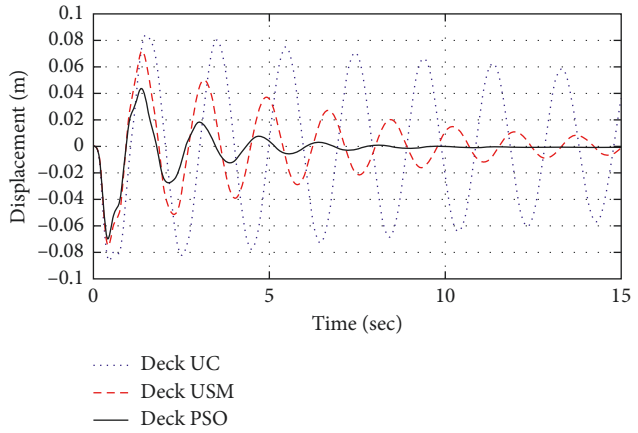

Figure 6: Deck displacement optimization case: deck displacement response.

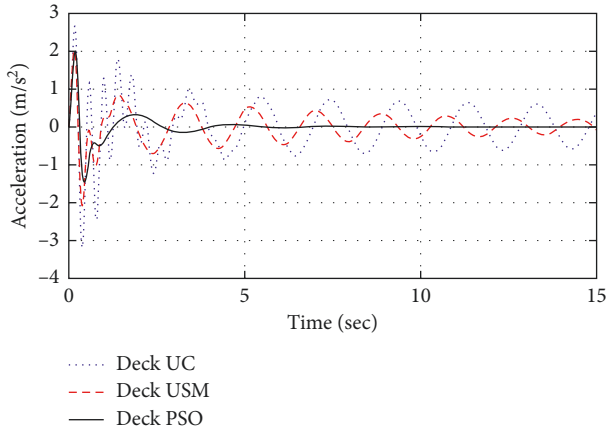

Figure 7: Deck acceleration optimization case: deck acceleration response.

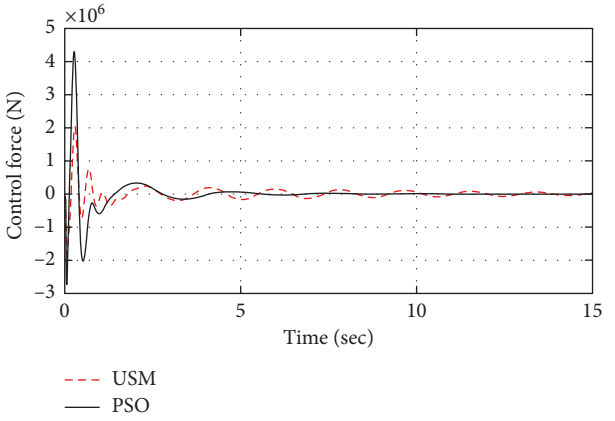

Figure 8: Deck acceleration optimization case: required control force.

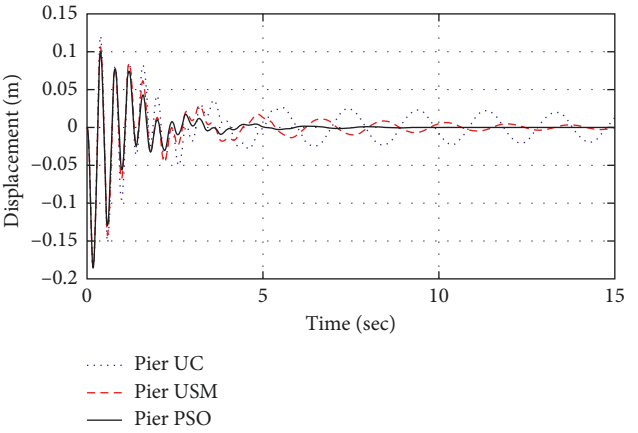

Figure 9: Deck displacement optimization case: resulting pier displacement response.

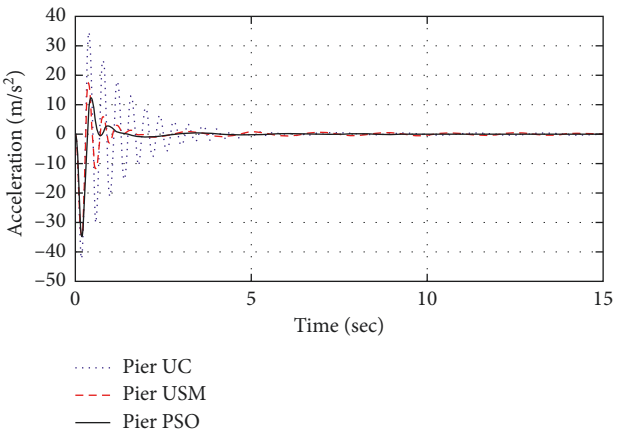

Figure 10: Deck acceleration optimization case: resulting pier acceleration response.

Table 4: Response reduction ratios for various optimization cases.

Optimization case	Method	Deck C_1	Deck C_2	Pier C_1	Pier C_2
Deck displacement	USM	0.87	0.67	1.01	0.85
	PSO	0.81	0.36	1.02	0.67
Deck acceleration	USM	0.65	0.67	0.81	0.37
	PSO	0.63	0.36	0.82	0.31
Pier displacement	USM	1.02	1.04	0.97	0.90
	PSO	1.11	1.18	0.93	0.89
Pier acceleration	USM	0.61	0.90	0.71	0.26
	PSO	0.47	1.09	0.44	0.13

configuration is not nearly as effective as minimizing deck response. These rows show that the minimization of pier displacement and acceleration typically comes with a significant increase in deck displacement and acceleration

response. For example, to use the PSO-PID results for pier displacement response reductions of $C_1 = 0.93$ and $C_2 = 0.89$, the performance indices for deck displacement increase to $C_1 = 1.11$ and $C_2 = 1.18$. This tradeoff is reasonable to expect because the dampers are connected between the top of the pier and the deck, and in this capacity, they are not situated between the impacted degree of freedom and the degree of freedom that is the object of the response minimization. Since the pier itself is impacted, the damper is not as effective at absorbing energy and reducing its response, especially just after impact, as it otherwise would be if it was located in a different configuration within the structure. This resulting deck displacement increase does not seem reasonable unless pier response minimization is deemed the highest priority for the design.

Table 5 shows the percentage decrease in response achieved by using the PSO technique instead of the USM. In this table, green indicates PSO outperforming the USM and orange indicates the converse statement.

Table 5 indicates that when optimizing for both deck displacement and acceleration responses, the PSO technique was better at finding optimum PID control gains that minimized deck responses. Once again, the tradeoff of better deck response for slightly worse pier peak response is seen, but only to a very small degree. This table also indicates that when optimizing for both pier displacement and acceleration response, the PSO technique outperforms the USM at finding optimum PID control gains that minimized pier responses. The better pier response-worse deck response tradeoff is also seen in these numbers. Table 5 is significant because it shows that using PSO over the USM for both deck displacement and acceleration, when measured by the energy performance index (C_2), leads to greater than 30% increases in response reduction. This demonstrates the importance of using a more rigorous PID tuning technique than the Ziegler–Nichols-based USM. It also demonstrates that for this impact load application, PSO is a very effective tuning technique for PID control gains.

Table 5: Benefits of using PSO over the USM.

Optimization case	Deck C_1	Deck C_2	Pier C_1	Pier C_2
Deck displacement	6.0%	30.9%	−0.8%	17.6%
Deck acceleration	2.6%	31.0%	−1.5%	5.9%
Pier displacement	−9.2%	−13.9%	3.9%	0.9%
Pier acceleration	14.0%	−19.1%	27.0%	12.7%

4. Summary and Conclusions

In order to investigate the effectiveness of smart structural control devices after high-impact events, a two degree-of-freedom highway bridge structure was modelled and its response simulated after an impact load. Control devices were attached to the structure between the bridge deck and pier degrees of freedom and used to minimize bridge deck response after impact. Both displacement and acceleration minimization were achieved using PID active control. In order to optimize PID control gains, the Ziegler–Nichols ultimate sensitivity method and Kennedy and Eberhart's particle swarm optimization method were used. In addition to demonstrating a minimization of structural response using PID control, the PSO technique was shown to be far superior to Ziegler–Nichols ultimate sensitivity method tuning rules for this impact load application. Using the ultimate sensitivity method, deck response reductions of greater than 13% and 33% were seen for displacement and acceleration responses, respectively, regardless of the performance index used to analyze them. Similarly, using PSO, deck response reductions of greater than 19% and 37% were seen for displacement and acceleration responses, respectively, regardless of the performance index used to analyze them. The direct comparison of USM to PSO indicated that when optimizing deck response, PSO is between 2.6% and 31% more effective than USM in minimizing response measured using the peak and energy performance indices. This indicates very effective structural control after impact loading and validates the use of PID control with PSO for the proposed application. In order to improve the performance of the PSO algorithm, many approaches could be used. For the current application, using a different population topology in order to better capture local optima in the design space is one potential improvement. Another potential improvement is to use a new objective function that features a shorter response time interval as its basis. In order to further study smart control for highway bridge structures after high-impact loads, a control force optimization scheme should be included with the above analysis. This should provide field implementable optimum results for PSO-PID control of small highway bridge structures.

Data Availability

The time-history data used to support the findings of this study are available from the corresponding author upon request.

Conflicts of Interest

The authors declare that they have no conflicts of interest.

Acknowledgments

The authors would like to thank research assistant Vivien Lefebvre of Ecole Nationale d'Ingénieurs de Saint Etienne, France, for his significant contribution to this project.

References

[1] H. Adeli and A. Saleh, "Integrated structural control optimization of large adaptive smart structures," *International Journal of Solids and Structures*, vol. 35, no. 28-29, pp. 3815–3830, 1997.

[2] Y. J. Cha, Y. Kim, and T. You, "Advanced sensing and structural health monitoring," *Journal of Sensor*, vol. 2018, Article ID 7286069, 3 pages, 2018.

[3] Y. Kim, P. Park, R. Sharifi, U. Berardi, and C. Kim, "System identification, health monitoring, and control design of smart structures and materials, Editorial," *Journal of Advanced Mechanical Engineering*, vol. 9, no. 4, article 1687814017699340, 2017.

[4] J. Hughes, Y. Kim, T. El-Korchi, and D. Cyganski, "Radar-based impact load prediction for damage mitigation of infrastructure," *Journal of Vibration and Control*, vol. 23, no. 12, pp. 1908–1924, 2015.

[5] M. D. Symans and M. C. Constantinou, "Semi-active control systems for seismic protection of structures: a state-of-the-art review," *Engineering Structures*, vol. 21, pp. 469–487, 1999.

[6] R. Mitchell, Y. J. Cha, Y. Kim, and A. Mahajan, "Active control of highway bridges subject to a variety of earthquake loads," *Earthquake Engineering and Engineering Vibration*, vol. 14, no. 2, pp. 253–263, 2015.

[7] Y. Kim, J. M. Kim, Y. H. Kim, J. W. Chong, and H. S. Park, "System identification of smart buildings under ambient excitations," *Journal of Measurement*, vol. 87, pp. 294–302, 2016.

[8] Y. Kim, S. Hurlebaus, and R. Langari, "Control of a seismically excited benchmark building using linear matrix inequality-based semiactive nonlinear fuzzy control," *Journal of Structural Engineering*, vol. 136, no. 8, pp. 1023–1026, 2010.

[9] Y. Kim, R. Langari, and S. Hurlebaus, "Model-based multi-input, multi-output supervisory semiactive nonlinear fuzzy controller," *Computer-Aided Civil and Infrastructure Engineering*, vol. 25, no. 5, pp. 387–393, 2010.

[10] Y. Kim, C. Kim, and R. Langari, "Novel bio-inspired smart control for hazard mitigation of civil structures," *Journal of Smart Materials and Structures*, vol. 19, no. 11, article 115009, 2010.

[11] S. K. Arsava and Y. Kim, "Modeling of magnetorheological dampers under various impact forces," *Shock and Vibration*, vol. 2015, Article ID 905186, 20 pages, 2015.

[12] S. K. Arsava, Y. Nam, and Y. Kim, "Nonlinear system identification of smart reinforced concrete structures under high impact loads," *Journal of Vibration and Control*, vol. 22, no. 16, 2015.

[13] S. K. Arsava, Y. Kim, K. H. Kim, and B. S. Shin, "Smart fuzzy control of reinforced concrete structures excited by collision-type forces," *Expert Systems with Applications*, vol. 42, no. 21, pp. 7929–7941, 2015.

[14] K. S. Arsava, Y. Kim, T. El-Korchi, and H. S. Park, "Nonlinear system identification of smart structures under high impact loads," *Smart Materials and Structures*, vol. 22, no. 5, article 055008, 2013.

[15] R. Mitchell, Y. Kim, and T. El-Korchi, "System identification of smart structures using a wavelet neuro-fuzzy model," *Journal of Smart Materials and Structures*, vol. 21, no. 11, article 115009, 2012.

[16] B. F. Spencer and S. Nagarajaiah, "State of the art of structural control," *Journal of Structural Engineering*, vol. 129, no. 7, pp. 845–856, 2003.

[17] O. Yoshida and S. J. Dyke, "Seismic control of a nonlinear benchmark building using smart dampers," *Journal of Engineering Mechanics*, vol. 130, no. 4, pp. 386–392, 2004.

[18] Y. Kim, R. Langari, and S. Hurlebaus, "Semiactive nonlinear control of a building structure equipped with a magneto-rheological damper system," *Mechanical Systems and Signal Processing*, vol. 23, no. 2, pp. 300–315, 2009.

[19] G. R. Consolazio and D. R. Cowan, "Nonlinear analysis of barge crush behavior and its relationship to impact resistant bridge design," *Computers and Structures*, vol. 81, no. 8–11, pp. 547–557, 2003.

[20] Y. J. Cha, A. K. Agrawal, Y. Kim, and A. Raich, "Multi-objective genetic algorithms for cost-effective distributions of actuators and sensors in large structures," *Expert Systems with Applications*, vol. 39, no. 9, pp. 7822–7833, 2012.

[21] Y. J. Cha, Y. Kim, A. Raich, and A. K. Agrawal, "Multi-objective optimization for actuator and sensor layouts of actively controlled 3D buildings," *Journal of Vibration and Control*, vol. 19, no. 6, pp. 942–960, 2013.

[22] Y. Kim, J. W. Bai, and L. D. Albano, "Fragility estimates of smart structures with sensor faults," *Journal of Smart Materials and Structures*, vol. 22, no. 12, article 125012, 2014.

[23] R. Mitchell, Y. Kim, T. El-Korchi, and Y. J. Cha, "Wavelet-neuro-fuzzy control of hybrid building-active tuned mass damper system under seismic excitations," *Journal of Vibration and Control*, vol. 19, no. 12, pp. 1881–1894, 2013.

[24] K. S. Park, H. M. Koh, S. Y. Ok, and C. W. Seo, "Fuzzy supervisory control of earthquake-excited cable-stayed bridges," *Engineering Structures*, vol. 27, no. 7, pp. 1086–1100, 2005.

[25] S. Yan and H. Zhang, "Smart vibration control analysis of seismic response using MR dampers in the elevated highway bridge structures," in *Proceedings of SPIE Smart Structures and Materials + Nondestructive Evaluation and Health Monitoring*, vol. 5765, pp. 1053–1060, San Diego, CA, USA, May 2005.

[26] B. Erkus, M. Abe, and Y. Fujino, "Investigation of semi-active control for seismic protection of elevated highway bridges," *Engineering Structures*, vol. 24, no. 3, pp. 281–293, 2002.

[27] Y. Li and J. Wang, "Experimental study on PID control of magnetorheological shock absorber under impact load," in *Proceedings of 15th International Congress on Sound and Vibration*, pp. 3022–3028, Daejeon, South Korea, July 2008.

[28] S. K. Arsava and Y. Kim, "A fuzzy controller for optimization of magnetic fields for reduction of impacts on coastal infrastructure," *Journal of Coastal Research*, 2016, In press.

[29] T. A. Hoang, K. T. Ducharme, Y. Kim, and P. Okumus, "Structural impact mitigation of bridge piers using tuned mass damper," *Engineering Structures*, vol. 112, pp. 287–294, 2016.

[30] S. El-Tawil, E. Severino, and P. Fonseca, "Vehicle collision with bridge piers," *Journal of Bridge Engineering*, vol. 10, no. 3, pp. 345–353, 2005.

[31] K. J. Åström and T. Hägglund, "The future of PID control," *Control Engineering Practice*, vol. 9, no. 11, pp. 1163–1175, 2001.

[32] R. Guclu, "Sliding mode and PID control of a structural system against earthquake," *Mathematical and Computer Modelling*, vol. 44, no. 1-2, pp. 210–217, 2006.

[33] J. G. Ziegler and N. B. Nichols, "Optimum settings for automatic controllers," *Transactions of the ASME*, vol. 64, pp. 759–768, 1942.

[34] P. Cominos and N. Munro, "PID controllers: recent tuning methods and design to specification," *IEEE Proceedings: Control Theory and Applications*, vol. 149, no. 1, pp. 46–53, 2002.

[35] J. Kennedy and R. Eberhart, "Particle swarm optimization," in *Proceedings of IEEE International Conference on Neural Networks IV*, pp. 1942–1948, Perth, Australia, November-December 1995.

[36] R. C. Eberhart and Y. Shi, "Comparison between genetic algorithms and particle swarm optimization," in *Proceedings of International Conference on Evolutionary Computation*, pp. 611–616, San Diego, CA, USA, March 1998.

[37] G. Venter and J. Sobieszczanski-Sobieski, "Particle swarm optimization," *AIAA Journal*, vol. 41, no. 8, pp. 1583–1589, 2003.

[38] R. Poli, J. Kennedy, and T. Blackwell, "Particle swarm optimization: an overview," *Swarm Intelligence Journal*, vol. 1, no. 1, pp. 33–57, 2007.

[39] P. J. Angeline, "Using selection to improve particle swarm optimization," in *Proceedings of International Conference on Evolutionary Computation*, pp. 84–89, Anchorage, AK, USA, 1998.

[40] J. Kennedy, *Particle Swarm Optimization, Encyclopedia of Machine Learning*, Springer, New York, NY, USA, 2010.

[41] M. Millonas, "Swarms, phase transitions, and collectiveintelligence," in *Proceedings of Artificial Life III: Proceedings of the Workshop on Artificial Life*, C. G. Langton, Ed., Addison Wesley, Santa Fe, NM, USA, June 1992.

[42] R. E. Perez and K. Behdinan, "Particle swarm approach for structural design optimization," *Computers and Structures*, vol. 85, no. 19-20, pp. 1579–1588, 2007.

[43] R. C. Eberhart and X. Hu, "Human tremor analysis using particle swarm optimization," in *Proceedings of IEEE International Conference on Evolutionary Computation*, Washington, DC, USA, 1999.

[44] G. Venter and J. Sobieszczanski-Sobieski, "Multidisciplinary optimization of a transport aircraft wing using particle swarm optimization," *Structural and Multidisciplinary Optimization*, vol. 26, no. 1-2, pp. 121–131, 2002.

[45] Z. Gaing, "A particle swarm optimization approach for optimum design of PID controller in AVR system," *IEEE Transactions on Energy Conversion*, vol. 19, no. 2, pp. 384–391, 2004.

[46] Y. Shi and R. Eberhart, "A modified particle swarm optimizer," in *Proceedings of IEEE International Conference on Evolutionary Computation*, pp. 69–73, IEEE Press, Piscataway, NJ, USA, 1998.

[47] P. Fourie and A. Groenwold, "The particle swarm optimization algorithm in size and shape optimization," *Structural Multidisciplinary Optimization*, vol. 23, no. 4, pp. 256–267, 2002.